HHS Public Access

Author manuscript

Angew Chem Int Ed Engl. Author manuscript; available in PMC 2017 February 18.

Published in final edited form as:

Angew Chem Int Ed Engl. 2016 February 18; 55(8): 2787–2791. doi:10.1002/anie.201511148.

Noninvasive Staging of Kidney Dysfunction Enabled by Renal Clearable Luminescent Gold Nanoparticles

Dr. Mengxiao Yu,
Department of Chemistry, The University of Texas at Dallas 800 W. Campbell Rd., Richardson, TX 75080 (USA)

Dr. Jiancheng Zhou,
Department of Urology, The University of Texas Southwestern Medical Center 5323 Harry Hines Blvd., Dallas, TX 75390 (USA)

Bujie Du,
Department of Chemistry, The University of Texas at Dallas 800 W. Campbell Rd., Richardson, TX 75080 (USA)

Xuhui Ning,
Department of Chemistry, The University of Texas at Dallas 800 W. Campbell Rd., Richardson, TX 75080 (USA)

Craig Authement,
Department of Urology, The University of Texas Southwestern Medical Center 5323 Harry Hines Blvd., Dallas, TX 75390 (USA)

Leah Gandee,
Department of Urology, The University of Texas Southwestern Medical Center 5323 Harry Hines Blvd., Dallas, TX 75390 (USA)

Prof. Dr. Payal Kapur,
Department of Pathology and Urology, The University of Texas Southwestern Medical Center 5323 Harry Hines Blvd., Dallas, TX 75390 (USA)

Prof. Dr. Jer-Tsong Hsieh, and
Department of Urology, The University of Texas Southwestern Medical Center 5323 Harry Hines Blvd., Dallas, TX 75390 (USA)

Prof. Dr. Jie Zheng[*]
Department of Chemistry, The University of Texas at Dallas 800 W. Campbell Rd., Richardson, TX 75080 (USA)

Department of Urology, The University of Texas Southwestern Medical Center 5323 Harry Hines Blvd., Dallas, TX 75390 (USA)

Abstract

[*] jiezheng@utdallas.edu.

Supporting information for this article is given via a link at the end of the document.

As a “silent killer”, kidney disease is often hardly detected at its early stage but can cause the lethal kidney failure in its late stage. Thus, a preclinical imaging technique that can readily differentiate the stages of kidney dysfunction is highly desired for fundamental understanding of kidney disease progression. Herein, we reported that *in vivo* fluorescence imaging, enabled by renal clearable near infrared-emitting gold nanoparticles, can noninvasively detect kidney dysfunction, report the dysfunctional stages and even reveal adaptive function in mouse model of unilateral obstructive nephropathy that cannot be diagnosed with routine kidney function markers. These results demonstrated that low-cost florescence kidney functional imaging is highly sensitive for longitudinal, noninvasive monitoring of kidney dysfunction progression in the preclinical research.

Keywords

Kidney disease; Kidney dysfunction; Fluorescence imaging; Imaging agents; Nanoparticles

Nearly 10% of adults worldwide are being influenced by a variety of kidney diseases that are often silent in the early stage but can cause the kidney failure in the late stage.[1] While typical markers such as blood urea nitrogen and creatinine have been routinely used for staging kidney dysfunctions, due to the high functional reservation of the kidney, these markers are often insensitive to kidney dysfunction at early stage and remain within the normal range even with the loss of 65-75% of the kidney function.[1a] To address this challenge, noninvasive *in vivo* imaging techniques such as single-photon emission computed tomography (SPECT), magnetic resonance imaging and computed tomography have been widely used to consecutively assess kidney dysfunction stages by real-time monitoring of kidney clearance kinetics (KCK) of renal clearable probes.[2] However, their high cost, low accessibility and potential risk of radiation exposure[3] have been limiting the advancement of fundamental understanding of kidney diseases in the preclinical research.

In vivo near-infrared fluorescence imaging is a low-cost, high-sensitivity and widely used preclinical tool for studying many diseases such as cancer.[4] However, fluorescence noninvasive imaging of kidney dysfunction and its stages has been a long-term challenge[5] due to low kidney-contrast enhancement and long-term nonspecific accumulation of organic dyes in the background tissues.[6] To address this long-standing challenge, we have recently applied renal clearable near-infrared-emitting glutathione-coated gold nanoparticles (GS-AuNPs) as contrast agent in the fluorescence imaging of KCK in normal mice.[6] We were able to noninvasively and fluorescently monitor KCK with a 50-fold increase of kidney-contrast enhancement over that obtained with conventional organic dyes. However, a fundamental question that whether such fluorescence imaging technique enabled by GS-AuNPs is sensitive enough to noninvasively detect kidney function changes and differentiate dysfunction stages like its radiological imaging counterparts is still unknown, but it is key to the future success of fluorescence imaging as a widely accessible preclinical tool in kidney function studies.

Using a unilateral ureteral obstruction (UUO) mouse model, a well-established preclinical model for ureteropelvic junction obstruction that is asymptomatic at an early stage but can

cause renal failure if not treated promptly in new borns,[5, 7] we found that time-fluorescence intensity curves (TFICs) derived from kidney clearance of renal clearable near-infrared-emitting GS-AuNPs were extremely sensitive to the impairments in kidney function, which were hardly detected with kidney function markers blood urea nitrogen and serum creatinine (**Table S1**). We not only directly identified the kidney with impaired function (reduced blood perfusion and decreased clearance) but also can differentiate dysfunction stages (a mild stage versus a severe stage) that were well consistent with renal damage levels evaluated by pathological analysis. Moreover, high sensitivity of fluorescence KCK even allowed detection of an adaptive function of the contralateral unobstructed kidney (increased blood perfusion and enhanced clearance) when the obstructed kidney was severely damaged. These results clearly indicated that with assistance of GS-AuNPs, noninvasive fluorescence imaging of KCK can serve as a low-cost, high-sensitivity and complementary tool for noninvasive staging of kidney dysfunction in preclinical animal models, which is expected to greatly expedite the advancement of our fundamental understanding of kidney diseases.

Near-infrared-emitting GS-AuNPs were synthesized with an approach we reported before.[8] The core size and hydrodynamic diameter of GS-AuNPs were 2.5 ± 0.3 nm and 3.3 ± 0.4 nm, respectively.[8] Since the hydrodynamic diameter of GS-AuNPs in native physiological environment is well below the kidney filtration threshold (6-8 nm), the NPs can be cleared out of the body through the kidneys with an efficiency comparable to those of clinically used small molecule-based contrast agents.[9] Different from near-infrared lipophilic organic fluorophores that severely accumulate in the background tissues, zw itterionic GS-AuNPs have extremely low accumulation in the background tissues;[6] thus, KCK of GS-AuNPs can be noninvasively and accurately monitored using *in vivo* fluorescence imaging.[6]

To investigate whether noninvasive fluorescence imaging of KCK enabled by renal clearable GS-AuNPs can report the kidney dysfunction, we tested KCK imaging in UUO mouse model, which was generated by complete ligation of the left ureter of mice while the right ureter was kept intact (**Figure 1A**). For sham-operated group the left ureters were exposed but not ligated. At 7-9 days post-operation, characteristic structural changes of kidney caused by obstruction were confirmed by *ex vivo* study (**Figure 1A**). However, the UUO mice and sham control showed no significant difference in the levels of blood urea nitrogen and serum creatinine, the most common biomarkers of renal function ($P > 0.05$, **Table S1**). This result was consistent with previous findings that blood urea nitrogen and serum creatinine are not good indicators of renal function in UUO model,[10] owing to the presence of a contralateral kidney that functions well.

With near-infrared-emitting GS-AuNPs as contrast agent, we easily differentiated the UUO left kidney (UUO LK) from the unobstructed kidneys with noninvasive images and TFICs (**Figure 1B-D** and **Figure S1,S2**) while IRDye 800CW failed to do it because intensive skin background overwhelmed the real kidney signal (**Figure S3**). At 1 min post intravenous injection of GS-AuNPs, the obstructed LK exhibited dramatically reduced fluorescence signals compared to contralateral right kidney (RK) in UUO mouse and kidneys in sham control (**Figure 1B, Figure S1**), corresponding to a remarkable decrease in the peak value (41.8% in average) compared with that of contralateral RK ($P < 0.05$, **Figure 2A** and **Table S2**). Such a diminished accumulation of contrast agent in UUO kidney indicated the blood

perfusion was dramatically reduced when obstruction occurred, consistent with previous findings in SPECT imaging of KCK of UUO mice.[11] The reduced blood perfusion of UUO LK resulted in unequal functional status of the two kidneys in UUO mice. In normal status the two kidneys have equal function because LK and RK in sham control showed ~50% in the percentage of relative renal function (% RRF = [peak value of LK or RK / (peak value of LK + peak value of RK)]×100%) (**Figure 2B** and **Table S2**). When obstruction happened in LK, the % RRF of UUO LK decreased to 36.1 ± 2.4 % (**Figure 2B**), in agreement with the % RRF of UUO LK obtained with SPECT imaging (34.6 ± 4.9 %).[5] Moreover, clearance of NPs through the kidney (defined as clearance percentage at 60 min = [(peak value – intensity at 60 min) / peak value]×100%; **Figure 1D**) declined from 44.1 ± 6.6 % in sham LK to 31.3 ± 6.0 % in UUO LK (**Figure 2C** and **Table S2**), also consistent with previous data reported in SPECT imaging of UUO model (clearance percentage at 20 min dropped from ~79.1% in sham control to ~13.7% in UUO kidney).[5] Furthermore, the differences in the peak time between sham control and UUO model became statiscially signficant, which will be discussed in the following section (**Figure 2D** and **Table S2**).

Not only the kidney with declined function but also the stages of kidney dysfunction can be differentiated by noninvasive fluorescence imaging of KCK. As shown in **Figure 3A**, we observed three different patterns of kidney TFICs in UUO model compared to that in shame model (pattern (a); **Movie S1**). In addition to the TFIC pattern we discussed above where the peak value of UUO kidney dramatically decreased (pattern (b); **Movie S2**), we also observed another type of TFIC pattern showing a relatively small reduction in peak value and a prolonged retention in the kidney (pattern (c); **Movie S3, Figure S4, Table S3**). Pathological analysis of kidney tissues revealed that these two different TFIC patterns can be correlated with two degrees of renal damage—a mild level where the renal tubules showed mild to moderate atrophy and dilatation (total pathological score of 2, **Table S4**) and a severe level where the renal tubular damage and cortical atrophy were much more pronounced (total pathological score of 4-6, **Table S4**) (**Figure 3B**, left column). In the mild stage, the peak value of UUO LK was slightly reduced compared with sham LK but excretion through the kidney was slowed down (**Figure 3A**, pattern (c)). This TFIC pattern of mild stage was consistent with data obtained in SPECT imaging of UUO at early stage (3 h post operation, technetium-99m mercaptoacetyltriglycine, ^{99m}Tc-MAG3, as contrast agent).[11] With the progression of renal damage into a severe level, TFIC pattern was changed to pattern (b): the peak value dramatically decreased and the kidney TFIC resembled the blood background (skin TFIC) in the profile (**Figure 3A**, **Figure 1D** and **Figure S2**), implying the kidney failure resulted from the severe injury.[12]

In addition to staging of kidney dysfunction, *in vivo* fluorescence imaging was also sensitive enough to detect adaptive function of contralateral RKs in UUO mouse model. Even though no structural changes were observed in contralateral RKs (**Figure 3B**, right column), a second decay phase of kidney TIFCs appeared during 15~60 min in UUO RK, following the initial decrease within ~15 min (**Figure 3A**, pattern (d)); whereas, at normal status, the decrease of kidney intensity ended at 20 min post injection (Sham LK, **Figure 3A**, pattern (a); Sham RK, **Figure 1C** and **Figure S2**). This two-phase decay contributed to a significant increase of clearance of GS-AuNPs through the RKs due to the injury of LKs: clearance

percentage at 60 min increased from 51.5 ± 4.9 % in sham control to 69.8 ± 3.0 % in UUO model ($P < 0.05$, **Figure 2C** and **Table S2**). The average peak value of RK in UUO model at severe stage was much higher than that in sham control (524.3 ± 56.9 versus 389.9 ± 109.7, **Figure 2A** and **Table S2**), suggesting an enhancement of blood perfusion. The % RRF of contralateral RK increased from the normal value of ~50% to 63.4 ± 2.4 % in UUO mice ($P < 0.05$, **Figure 2B** and **Table S2**). The first peak appeared earlier than that of sham RK (1.7 ± 0.2 min versus 2.9 ± 0.4 min, $P < 0.05$, **Figure 2D** and **Table S2**), further indicating enhanced excretion of GS-AuNPs through the healthy RKs of UUO mice.

In summary, enabled by GS-AuNPs, *in vivo* fluorescence imaging technique can be sensitive enough to differentiate the normal function, mild dysfunction, severe dysfunction, and even adaptive function of kidney in UUO mice (**Figure 4**), which are hardly evaluated using conventional markers such as blood urea nitrogen and serum creatinine. Such high sensitivity in the evaluation of kidney dysfunction originated from high-contrast imaging of KCK of renal clearable near-infrared-emitting GS-AuNPs, which allows rich information of kidney function such as blood perfusion, relative functional status of the two kidneys and the clearance capability to be quantitatively extracted from kidney TFICs.

It should also be noted that GS-AuNP TFICs of UUO kidneys were not completely identical to the time-activity curves obtained with ^{99m}Tc-MAG3 as contrast agent in the SPECT kidney imaging: after reaching the peak value, a decay phase was observed from GS-AuNPs based TIFCs (**Figure 3A**, pattern (b); **Figure S2**) while the signal was maintained at a constant level from ^{99m}Tc-MAG3 based activity curves.[11] Such difference implied that renal excretion mechanism of GS-AuNPs is likely different from that of ^{99m}Tc-MAG3 (predominantly excreted by tubular secretion). Fluorescence microscopy imaging of kidney sections revealed that GS-AuNPs were mainly distributed in the glomeruli at 5 min post injection (**Figure S5**), suggesting that glomerular filtration was likely a major clearance route of GS-AuNPs. However, how exactly GS-AuNPs are filtrated through glomeruli needs further investigation. Moreover, pathological analysis of kidneys in sham mice revealed no structural alterations after intravenous injection of GS-AuNPs (**Figure 3B**), suggesting low renal toxicity of GS-AuNPs. Nevertheless, the results presented in this study suggested that *in vivo* fluorescence imaging could serve a powerful and sensitive preclinical kidney function imaging tool and advance our fundamental understanding of kidney disease progression.

Supplementary Material

Refer to Web version on PubMed Central for supplementary material.

Acknowledgements

This study was supported by the NIH (1R01DK103363), CPRIT (RP140544) and the start-up fund from the University of Texas at Dallas. We thank Chao-Long Huang, C. Mohan and Y. Du for insightful discussions.

References

1. a Star RA. Kidney Int. 1998; 54:1817–1831. [PubMed: 9853246] b Chawla LS, Eggers PW, Star RA, Kimmel PL. N. Engl. J. Med. 2014; 371:58–66. [PubMed: 24988558]

2. a Taylor AT. J. Nucl. Med. 2014; 55:608–615. [PubMed: 24549283] b Grenier N, Basseau F, Ries M, Tyndal B, Jones R, Moonen C. Abdom. Imaging. 2003; 28:164–175. [PubMed: 12592462] c Krier JD, Ritman EL, Bajzer Z, Romero JC, Lerman A, Lerman LO. Am. J. Physiol. Renal. Physiol. 2001; 281:F630–F638. [PubMed: 11553509]

3. Weissleder R, Pittet MJ. Nature. 2008; 452:580–589. [PubMed: 18385732]

4. a Kairdolf BA, Smith AM, Stokes TH, Wang MD, Young AN, Nie SM. Annu. Rev. Anal. Chem. 2013; 6:143–162.b Hyun H, Owens EA, Wada H, Levitz A, Park G, Park MH, Frangioni JV, Henary M, Choi HS. Angew. Chem. Int. Ed. 2015; 54:8648–8652.Angew. Chem. 2015; 127:8772–8776.c Perrault SD, Chan WCW. Proc. Natl. Acad. Sci. U. S. A. 2010; 107:11194–11199. [PubMed: 20534561]

5. Penna FJ, Chow JS, Minnillo BJ, Passerotti CC, Barnewolt CE, Treves ST, Fahey FH, Dunning PS, Freilich DA, Retik AB, Nguyen HT. J. Urol. 2011; 185:2405–2413. [PubMed: 21511294]

6. Yu MX, Liu JB, Ning XH, Zheng J. Angew. Chem. Int. Ed. 2015; 54:15434–15438.Angew. Chem. 2015; 127:15654–15658.

7. a Decramer S, Wittke S, Mischak H, Zurbig P, Walden M, Bouissou F, Bascands JL, Schanstra JP. Nat. Med. 2006; 12:398–400. [PubMed: 16550189] b Ulman I, Jayanthi VR, Koff SA. J. Urol. 2000; 164:1101–1105. [PubMed: 10958752]

8. Liu JB, Yu MX, Zhou C, Yang SY, Ning XH, Zheng J. J. Am. Chem. Soc. 2013; 135:4978–4981. [PubMed: 23506476]

9. a Zhou C, Long M, Qin YP, Sun XK, Zheng J. Angew. Chem. Int. Ed. 2011; 50:3168–3172.Angew. Chem. 2011; 123:3226–3230.b Zhou C, Hao GY, Thomas P, Liu JB, Yu MX, Sun SS, Oz OK, Sun XK, Zheng J. Angew. Chem. Int. Ed. 2012; 51:10118–10122.Angew. Chem. 2012; 124:10265–10269.c Yu MX, Zheng J. ACS Nano. 2015; 9:6655–6674. [PubMed: 26149184]

10. Chung S, Yoon H, Kim S, Kim S, Koh E, Hong Y, Park C, Chang Y, Shin S. Nutr. Metab. 2014; 11:2.

11. Tantawy MN, Jiang R, Wang F, Takahashi K, Peterson TE, Zemel D, Hao C-M, Fujita H, Harris RC, Quarles CC, Takahashi T. BMC Nephrol. 2012; 13:168. [PubMed: 23228112]

12. Fommei E, Ghione S, Hilson AJW, Mezzasalma L, Oei HY, Piepsz A, Volterrani D. Eur. J. Nucl. Med. 1993; 20:617–623. [PubMed: 8370384]

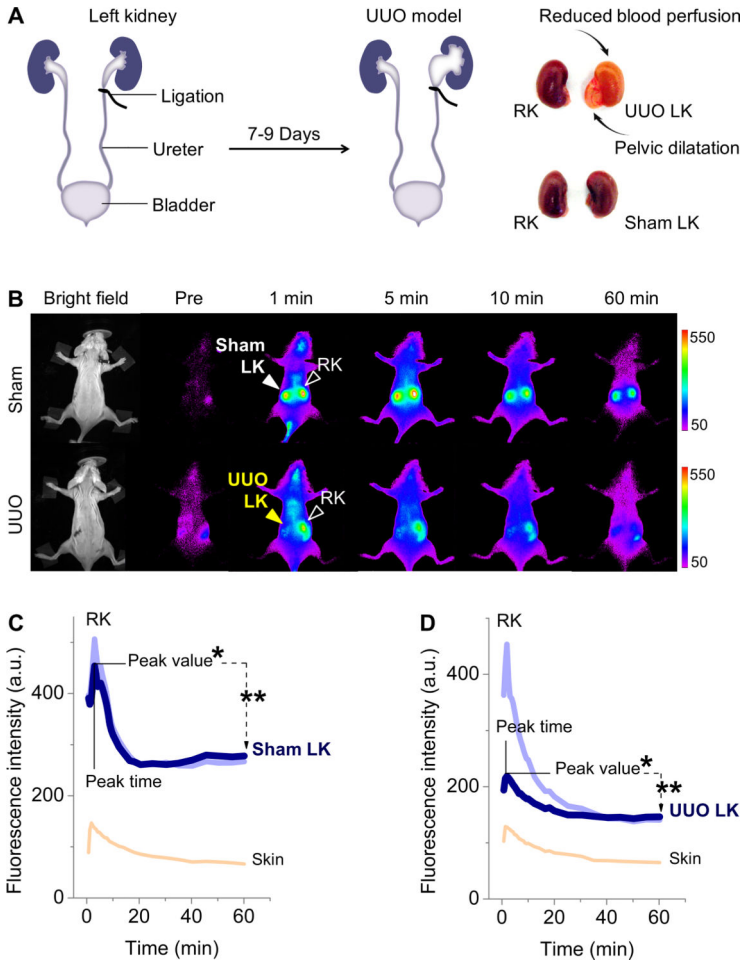

Figure 1.

(A) Unilateral ureteral obstruction (UUO) in mice was generated by complete ligation of the left ureter while the right ureter was kept intact. For sham-operated group the left ureters were exposed but not ligated. (B) Representative whole-body noninvasive fluorescence images of mice before and after intravenous injection of GS-AuNPs (Ex/Em filters: 710/830 nm). (C,D) Time-fluorescence intensity curves (TFICs) of kidneys in sham control (C) and UUO model (D). Four parameters were extracted from kidney TFICs: peak value, peak time = peak time of the first peak, *percentage of relative renal function (% RRF = [peak value of left kidney (LK) or right kidney (RK) / (peak value of LK + peak value of RK)]×100%), **clearance percentage at 60 min = [(peak value – intensity at 60 min) / peak value]×100%.

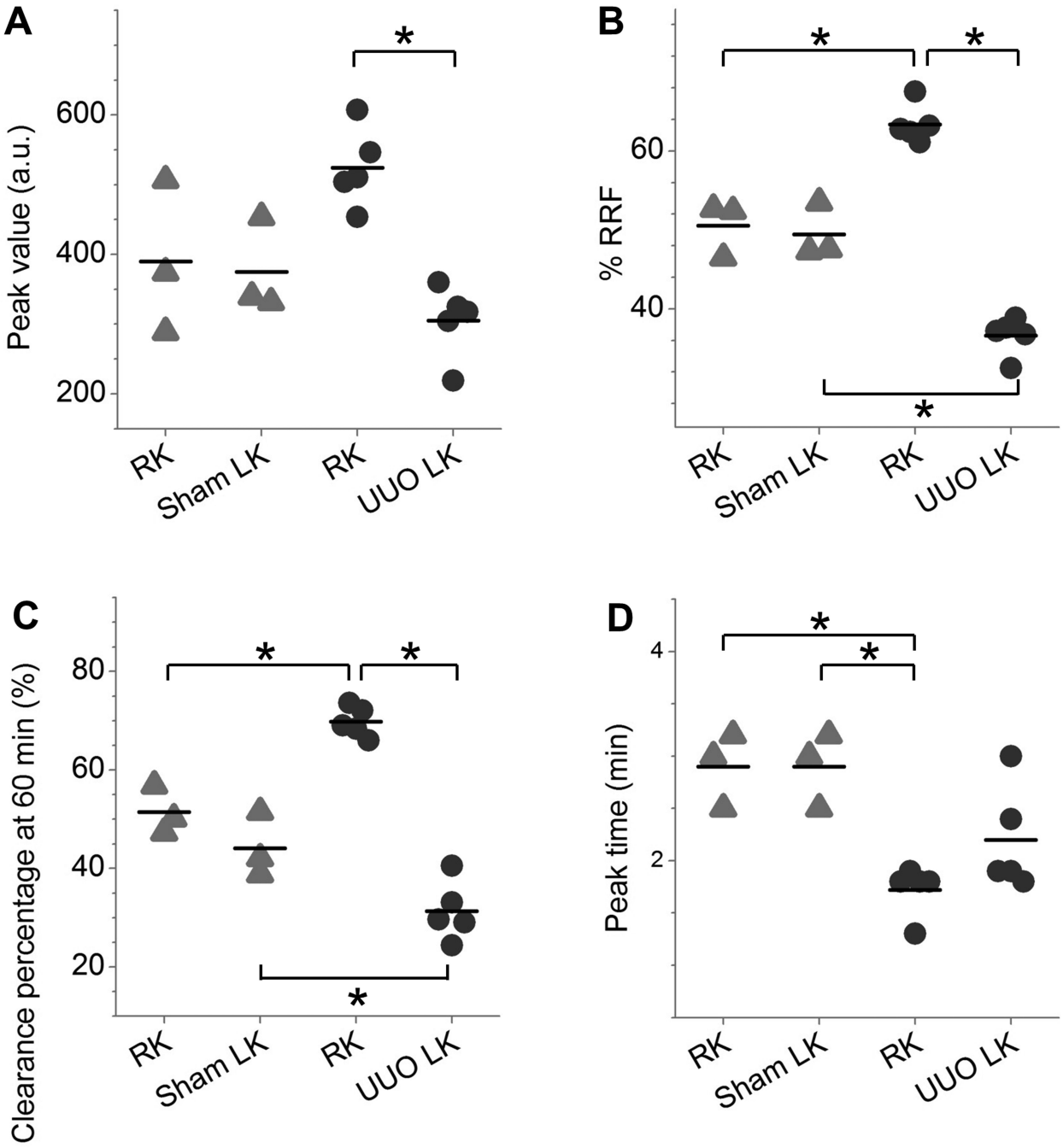

Figure 2.

Statistical analysis of four parameters extracted from kidney TFICs of UUO mice and sham control. The parameters included (A) peak value, (B) percentage of relative renal function (% RRF), (C) clearance percentage at 60 min, and (D) peak time. Sham control, triangle; UUO model, circle. LK, left kidney; RK, right kidney. N = 5 for UUO mice, N = 3 for sham control. Mean values were displayed. *P < 0.05.

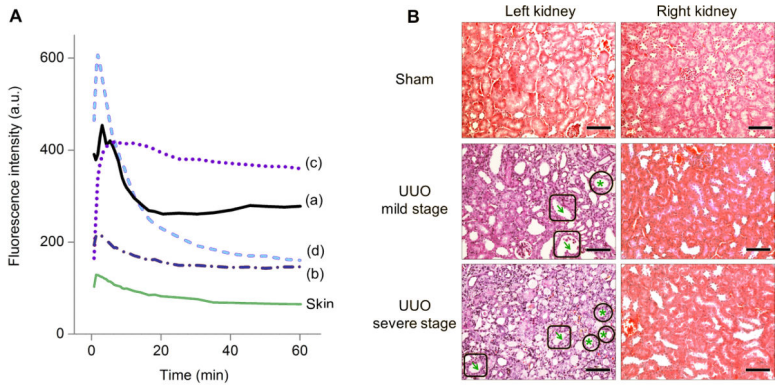

Figure 3.

Correlation of time-fluorescence intensity curve (TFIC) patterns with the degrees of renal damage. (A) Representative TFICs of sham left kidney (sham LK) (a), UUO LKs (b, c), and UUO model's right kidney (RK in UUO, d), corresponding to four statuses of kidney function: (a) normal function, (c) mild dysfunction, (b) severe dysfunction, and (d) adaptive function. Skin TFIC was obtained from the same mouse showing pattern (b) of UUO LK. (B) Pathologic analysis of kidneys of UUO mice and sham control (H&E stain, scale bar = 100 μm). Arrows in square: tubular dilatation; stars in circle: tubular atrophy. Nucleus was stained in violet and cytoplasm was stained in pink. From sham LK to UUO LKs, the color change from pink to violet reflected a loss of cytoplasm, the characteristic of cellular atrophy. RKs were normal.

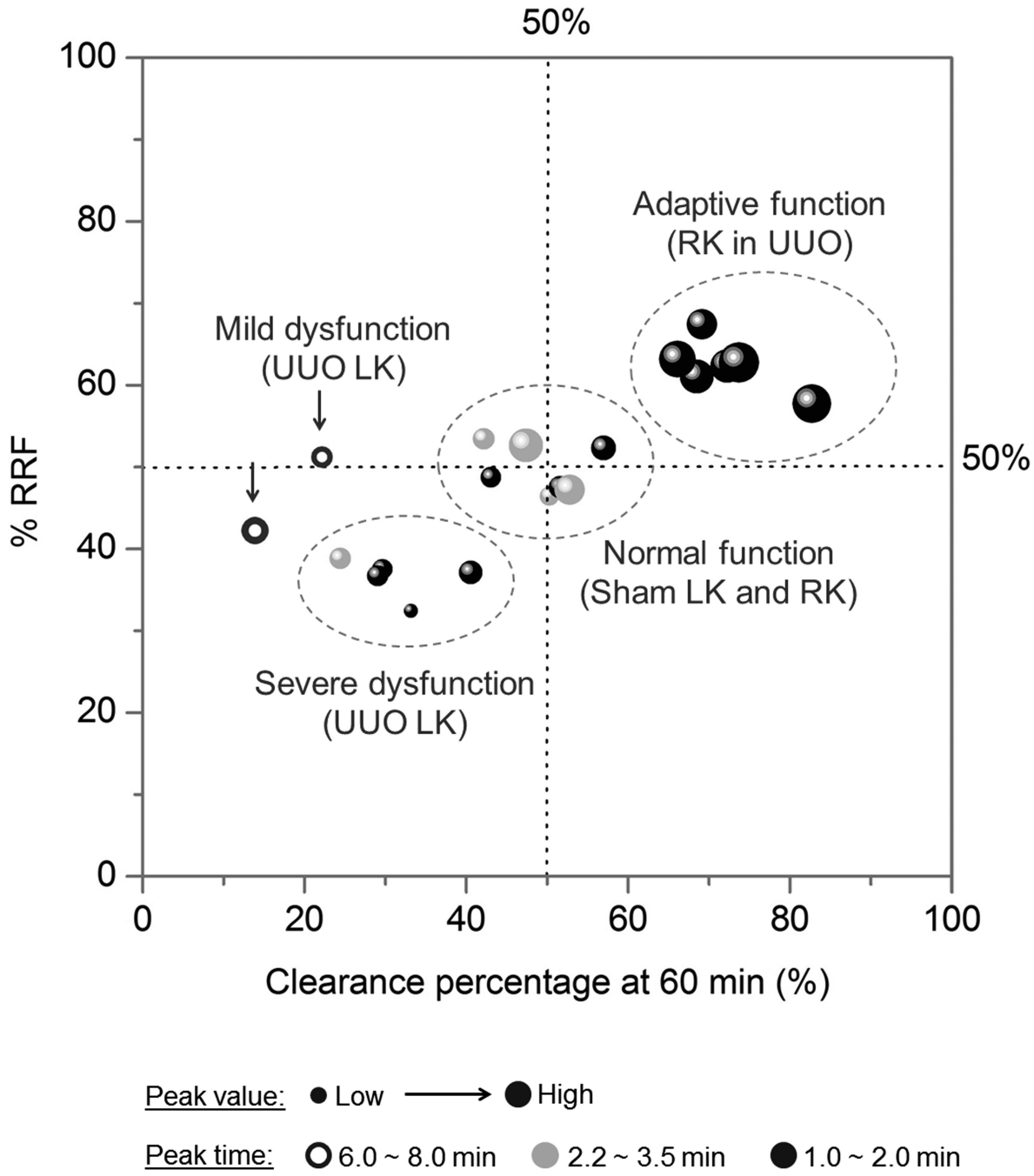

Figure 4.

Four functional statuses of kidney in UUO model can be clearly differentiated by plotting the four parameters of TFICs in one figure. X = clearance percentage at 60 min, Y = % RRF, bubble size = peak value, bubble color = peak time (black, 1.0 ~ 2.0 min; gray , 2.2 ~ 3.5 min; hollow circle, 6.0 ~ 8.0 min). Data were obtained from 20 kidneys in 10 mice and presented in Table S2 and S3 (N = 7 for UUO model; N = 3 for sham control).